RESEARCH ARTICLE

Cross-species reactivity of antibodies against *Plasmodium vivax* blood-stage antigens to *Plasmodium knowlesi*

Fauzi Muh[1], Namhyeok Kim[1], Myat Htut Nyunt[2], Egy Rahman Firdaus[1], Jin-Hee Han[1], Mohammad Rafiul Hoque[1], Seong-Kyun Lee[1], Ji-Hoon Park[1], Robert W. Moon[3], Yee Ling Lau[4], Osamu Kaneko[5], Eun-Taek Han[1]*

1 Department of Medical Environmental Biology and Tropical Medicine, School of Medicine, Kangwon National University, Chuncheon, Gangwon-do, Republic of Korea, **2** Department of Medical Research, Yangon, Republic of Myanmar, **3** Department of Infection Biology, Faculty of Infectious and Tropical Diseases, London School of Hygiene and Tropical Medicine, London, United Kingdom, **4** Department of Parasitology, Faculty of Medicine, University of Malaya, Kuala Lumpur, Malaysia, **5** Department of Protozoology, Institute of Tropical Medicine (NEKKEN), Nagasaki University, Sakamoto, Nagasaki, Japan

* etaekhan@gmail.com.

Abstract

Malaria is caused by multiple different species of protozoan parasites, and interventions in the pre-elimination phase can lead to drastic changes in the proportion of each species causing malaria. In endemic areas, cross-reactivity may play an important role in the protection and blocking transmission. Thus, successful control of one species could lead to an increase in other parasite species. A few studies have reported cross-reactivity producing cross-immunity, but the extent of cross-reactive, particularly between closely related species, is poorly understood. *P. vivax* and *P. knowlesi* are particularly closely related species causing malaria infections in SE Asia, and whilst *P. vivax* cases are in decline, zoonotic *P. knowlesi* infections are rising in some areas. In this study, the cross-species reactivity and growth inhibition activity of *P. vivax* blood-stage antigen-specific antibodies against *P. knowlesi* parasites were investigated. Bioinformatics analysis, immunofluorescence assay, western blotting, protein microarray, and growth inhibition assay were performed to investigate the cross-reactivity. *P. vivax* blood-stage antigen-specific antibodies recognized the molecules located on the surface or released from apical organelles of *P. knowlesi* merozoites. Recombinant *P. vivax* and *P. knowlesi* proteins were also recognized by *P. knowlesi*- and *P. vivax*-infected patient antibodies, respectively. Immunoglobulin G against *P. vivax* antigens from both immune animals and human malaria patients inhibited the erythrocyte invasion by *P. knowlesi*. This study demonstrates that there is extensive cross-reactivity between antibodies against *P. vivax* to *P. knowlesi* in the blood stage, and these antibodies can potently inhibit in vitro invasion, highlighting the potential cross-protective immunity in endemic areas.

Author summary

In recent years, malaria initiatives have increasingly shifted focus from achieving malaria control to achieving malaria elimination. However, the interventions used are leading to drastic changes in the proportions of different *Plasmodium* species causing clinical infection, particularly within Southeast Asia. Little is known about how these different parasite species interact/compete in nature or whether exposure to one species could cause some level of protection against another. We examined cross-reactive antibody responses to key parasite proteins with roles in red blood cell invasion and identified novel cross-species reactivity among the closest of malaria affecting the human population (*P. vivax* and *P. knowlesi*). This comprehensive analysis provides evidence that cross-reactive immunity could play an important role in areas where species distributions are perturbed by malaria control measures, and future efforts to identify the specific cross-reactive epitopes involved would be invaluable both to our understanding of malaria immunity and vaccine development.

Introduction

Malaria remains a deadly scourge in humans, with over 200 million cases and close to a half-million deaths reported annually [1]. Protozoan malaria parasites are transmitted by sporozoite inoculation by a mosquito vector into the human [2]. Five *Plasmodium* species infect humans; *Plasmodium falciparum*, *P. vivax*, *P. ovale*, *P. malariae*, and zoonotic malaria parasite *P. knowlesi* [2,3]. *P. falciparum* is the most virulent species and leads to most severe cases in Africa, while *P. vivax* is widely distributed and predominates in regions of Southeast Asia and South America [1]. Recently, a monkey malaria parasite, *P. knowlesi*, has been found to be cause a significant number of human infections in Southeast Asian countries [4–7].

In recent years, malaria initiatives have increasingly shifted focus from achieving malaria control to achieving malaria elimination. Interventions are leading to drastic changes in the proportions of different *Plasmodium* species affecting populations. For example, as *P. vivax* forms latent hypnozoite stages, infection rates are often slower to decline under control measures that *P. falciparum* [8]. In most areas where malaria is endemic, two or more human parasites coexist [9], and mixed infections with three malaria parasite species (*P. falciparum*, *P. vivax*, and *P. knowlesi*) have been identified in southern Myanmar, Thailand and Sabah, Malaysia [10–12]. However, little is known about how the different parasite species interact/compete in nature or whether exposure to one species could cause some level of protection against another. If cross-species immunity is important, the successful control of one species could lead to increases in the frequency or severity of infections from other *Plasmodium* species [9,13]. Previous studies looking at patients concurrently infected with multiple *Plasmodium* species demonstrated clear cross-regulatory patterns, including evidence for density-dependent regulation of parasitaemia and peak parasitaemias for each parasite forming sequential patterns [14]. Density-dependent regulation of parasitemia and specific immune responses targeting particular antigens could explain the prevalence of coinfection patterns in endemic areas [14].

An extreme example of how malaria control can affect species distribution is in Malaysia, where successful control of human malaria has led to a significant decline in *P. falciparum* and *P. vivax* cases at the same time as zoonotic *P. knowlesi* cases have dramatically increased. For example, in Sabah, *P. knowlesi* caused less than 5% of malaria cases in 2004, but in 2017, it was responsible for 98% of cases [15,16]. Equally, it is also possible that the removal of *P.*

falciparum or *P. vivax* from populations could have an effect on the spread or pathogenicity of other human parasites such as *P. ovale* and *P. malariae* which often cause subclinical infections [17].

However, cross-species immunity in malaria has been largely ignored in the last few decades [14]. Previous reports have observed cross-reactivity between *P. falciparum* and *P. malariae* and between *P. falciparum* and *P. vivax* due to conserved/homologous plasmodial proteins and the presence of shared B- and T-cells epitopes [18–25]. *P. vivax* antigens were recognized by sera from *P. vivax* and *P. falciparum* clinical patients [20,22]. Naturally acquired antibodies in *P. falciparum*-infected patients inhibit the invasion of hepatocytes by rodent malaria sporozoites [18]. Previous reports found that past exposure to *P. vivax* or *P. malariae* leads to lower morbidity and mortality following *P. falciparum* exposure [14,26]. However, little is known about which factors affect the cross-reactivity observed in those previous reports. In addition, the identification of species-transcending inhibitory antibodies could provide a powerful tool for vaccine development, particularly as these antibodies are far more likely to result in strain-transcending effects, which has been a major challenge in malaria vaccine research [27].

P. knowlesi and *P. vivax* are phylogenetically closely related [28], and approximately 89% of *P. vivax* genes have orthologues in *P. knowlesi* [29]. In silico analysis has demonstrated that there is a high degree of homology among plasmodial proteins, especially those of *P. vivax*, *P. knowlesi* and *P. cynomolgi* [28]; thus, cross-reactivity may play an important role in the prevalence patterns observed in endemic areas of Southeast Asian countries where both human and primate malaria coexist. It also remains interesting to explore the existence of cross-reacting epitopes in blood-stage malaria vaccine candidates including *P. knowlesi* [30]. The disease dynamic change has been seen in Malaysia while decreasing human *Plasmodium* species is observed, the increasing of *P. knowlesi* infection is inevitable [15]. The possibility of waning cross-protective *P. vivax* antibodies may contribute to increased zoonotic *Plasmodium* infection [31]. It is in line with our previous study that *P. vivax* antibodies inhibited the *P. knowlesi* invasion in vitro [25].

This study presents a systematic analysis of cross-species reactivity of antibodies against *P. vivax* blood-stage antigens and their inhibition activities against human erythrocyte invasion by *P. knowlesi*. We also observed that antigen-specific IgG antibodies from *P. vivax*-infected patients could inhibit erythrocyte invasion in *P. knowlesi* parasites. These data indicate that significant cross-species reactive antibodies are generated during malaria infections and that these may play a role in susceptibility or pathogenicity, particularly between closely related species like *P. vivax* and *P. knowlesi*. It suggests that the potential for a developed vaccine against multiple *Plasmodium* species should be examined in more detail.

Materials and methods

Ethics statement

Blood samples were taken from human subjects, age 18–70 years old after written-informed consent was obtained from all subjects. All experimental protocols involving human samples were approved by the Kangwon National University Hospital Ethical Committee (IRB No. 2014-08-008-002), the University of Malaya Medical Ethics Committee (Ref No. 817.18), and the Medical Research Ethics Committee (MREC), Ministry of Health, Malaysia (National Medical Research register ID No. 13079), in accordance with relevant guidelines and regulations. Blood samples were collected from *P. knowlesi*-infected patients in EDTA-vacutainer tubes provided by the University of Malaya Medical Center (UMMC), Malaysia during 2010–2013, on the day when the patients were positively diagnosed with malaria. All *P. knowlesi*

samples used for this study were confirmed by species-specific PCR as described elsewhere [4]. The patients' serum were collected from symptomatic patient visiting at endemic areas of Malaysia with parasitemia 0.207% in average (ranging from 0.003 to 1.380%) and age 38 years in average (range from 6 to 72). However, we did not obtain information about history of previous malaria infection from patients. *P. vivax*-infected patients were recruited from a *P. vivax*-endemic area in Gangwon province, the Republic of Korea (ROK) where *P. vivax* is major *Plasmodium* species, there is no *P. knowlesi* infection in this area [1]. Patients with *P. falciparum* infection were excluded in this study. The sera were collected from symptomatic patient visiting at local health centers and clinics in Gangwon Province, ROK with parasitemia ranging from 0.027 to 0.630%, mean 0.121%) and age 18 to 60 years (mean 28). *P. vivax* and *P. knowlesi* eight patient serum samples were pooled after species-specific PCR and eight health individuals without any *Plasmodium* infection. A total 70 individual *P. vivax*-, *P. knowlesi*-infected patients serum and health individuals were used for individual immunoscreening after preliminary pooled-serum screening. Patients without malaria were recruited from a population of healthy individuals living in nonendemic areas of the ROK; malaria negativity was confirmed by microscopy and PCR.

Sequence analysis of amino acid identity

The target antigens were selected from our previous studies that were localized in different apical organelles/ merozoite surface of *P. vivax* and were recognized by human patients serum (Table 1, see references). Amino acid sequences of *P. vivax* (Sal I and P01 strains) and *P. knowlesi* (H strain) were retrieved from PlasmoDB (www.plasmodb.org) [32] and aligned. Clustal W program was used to make a pairwise alignment to determine the percent amino acid identity (Table 1 and S1 Fig).

In vitro culture of blood-stage *P. knowlesi* parasites

The human-adapted *P. knowlesi* A1-H.1 strain was maintained with fresh human erythrocytes in RPMI 1640-based medium (Invitrogen/Life Technologies, Grand Island, NY) as described previously [53].

Recombinant protein expression

P. vivax recombinant proteins were generated by wheat germ cell-free or *E. coli* expression systems in our previous studies [25,42,44,50]. DNA fragments encoding PvRBP1a-34, Pv41, or PvRhopH2 were amplified from a Korean vivax isolate with primers PvRBP1a-34_F (ggtcgcg gatccgaattcATGAACGAACTAGGTATAGACATT) and PvRBP1a-34_R (ggtggtggtgctcgag TTCAAACTCTATCTTCAGTTC); Pv41_F (ggtcgcggatccgaattcATGGAACACATCTGCGAT TTTAC) and Pv41_R (ggtggtggtgctcgagCTCCTGGAAGGACTTGGCA); and PvRhopH2_F (ggtcgcggatccgaattcATGGAGCTGAGCCACAGC) and PvRhopH2_R (ggtggtggtgctcgag CTTCTCCACATCCTCGTGGT), respectively. Small letters indicate the plasmid-derived sequence and underlined letters indicate enzyme restriction sites, EcoRI and XhoI, respectively. High fidelity KOD-plus kit (Toyobo Co., Osaka, Japan) was used with an initial denaturation step at 94˚C for 2 min, followed by 35 cycles of 94˚C for 15 sec, 60˚C for 30 sec, and 58˚C for 1.5 min and a final extension step at 68˚C for 10 min. The amplicons were purified using a gel extraction kit and ligated into the pET28a(+) expression vector (Novagen, Madison, WI) for PvRBP1a-34 or the pET23a(+) expression vector for Pv41 and PvRhopH2 with a His-tag. Correctly ligated plasmids were transformed into *E. coli* BL21(DE3) pLysS (Life Technologies) for recombinant protein expression. Recombinant protein expression was induced with

Table 1. Characterization of *P. vivax* blood-stage antigen-specific antibodies, colocalization and the degree of similarity of homologous domains.

	P. vivax Sal-I				*P. knowlesi* strain H				
Name	PlasmoDB ID (Sal-I)	MW (full length/ functional domain)	Localization	Ref.	PlasmoDB ID	% identity (aa.) of functional domain with two *P. vivax* strains		Colocalization	Ref
						Sal-I	P01		
PvMSP1P	PVX_099975	214.6/9.6	Surface	[33]	PKNH_0728800	86.0	87.5	Surface	[34]
PvMSP1	PVX_099980	196.1/9.8	Surface	[35]	PKNH_0728900	82.0	87.4	Surface	[36]
PvMSP10	PVX_114145	52.3/47.0	Surface	[37]	PKNH_1129800	62.4	63.0	Surface	[38]
PvMSP8	PVX_097625	54.7/49.3	Surface	[39]	PKNH_1031500	82.8	84.1	ND	[38]
Pv41	PVX_000995	44.1/41.7	Surface	[40]	PKNH_0303000	83.7	83.7	Surface	[41]
Pv50	PVX_087140	50.4/48.4	Surface	[42]	PKNH_0730000	58.2	57.8	Surface	-
Pv32	PVX_084815	32.6/26.7	Surface	[43]	PKNH_0421000	77.3	76.8	Surface	-
PvMSA180	PVX_094920	182.1/43.0 (N) 57.9 (C)	Surface (N & C)	[44]	PKNH_0814000	61.8 (N) 74.5 (C)	61.6 (N) 74.9 (C)	Surface (N & C)	-
PvGAMA	PVX_088910	82.7/57.5	Microneme	[45]	PKNH_1322900	82.4	82.5	Microneme	-
PvDBP	PVX_110810	119.7/38.5	Microneme	[46]	PKNH_0623500	71.4	70.7	ND	[47]
PvAMA1	PVX_092275	64.5/64.5	Microneme	[42]	PKNH_0931500	85.4	85.0	Microneme	[47]
PvRBP1a	PVX_098585	326.3/34.4	Microneme	[48]	PkNBPXa PKNH_1472300 PkNBPXb PKNH_0700200	22.9 (Xa) 22.3 (Xb)	20.2 (Xa) 24.3 (Xb)	Microneme	-
PvRBP1b	PVX_098582	303.7/32.0	Microneme	[48]	PkNBPXa PKNH_1472300 PkNBPXb PKNH_0700200	26.9 (Xa) 31.3 (Xb)	16.7 (Xa) 14.6 (Xb)	Microneme	-
Pv12	PVX_113775	41.1/36.0	Rhoptry neck	[49]	PKNH_1137300	74.9	75.2	Rhoptry	NA
PvRON2	PVX_117880	244.6/68.9	Rhoptry neck	[42]	PKNH_1230100	71.0	78.0	ND*	NA
PvRAMA	PVX_087885	81.3/27.9	Rhoptry body	[50]	PKNH_0105800	74.6	75.6	ND**	NA
PvRhopH2	PVX_099930	160.9/42.6	Rhoptry body	[51]	PKNH_0727900	73.3	71.2	Rhoptry	NA
PvETRAMP 11.2	PVX_003565	11.9/9.5	PVM	[52]	PKNH_0418600	74.7	80.2	ND	NA
PvEXP1	PVX_091700	15.0/12.7	PVM	[52]	PKNH_0919300	77.5	79.6	ND	NA

Identity of amino acid sequences was obtained based on the alignment of the target region shown in S1 Fig and colocalization on *P. knowlesi* parasites was determined by the r^2 value (>70%) in S1 Table.

MW, predicted molecular weight; FL, full length; NA, not assigned; ND: not defined; PVM, parasitophorous vacuole membrane; N, N-terminal; and C, C-terminal.

*, probably on the rhoptry neck

**, not in the rhoptry bulb.

0.1 mM isopropyl-β-D-thiogalactopyranoside (IPTG; Sigma-Aldrich, St. Louis, MO). All recombinant proteins were solubilized, purified, and refolded as described elsewhere [47,54].

Meanwhile, *P. knowlesi* recombinant proteins were expressed for this study using wheat germ cell-free system for immunoscreening using specific primers (S2 Table), the procedures were described elsewhere[47]. Recombinant PkDBPα protein expression was described elsewhere [47]. The DNA fragment encoding PkRhopH2 was amplified from *P. knowlesi* A1-H.1 genomic DNA with primer pair PkRhopH2_F (ggtcgcggatccgaattcATGGAGTTAGGCCATACCGTG) and PkRhopH2_R (ggtggtggtgctcgagCTTCTCGATGTCTTCGTAGTCCA). Lowercase letters indicate the plasmid-derived sequence and underlined letters indicate the enzyme restriction sites for EcoRI and XhoI, respectively. A high fidelity KOD-plus kit was

used with an initial denaturation step at 94˚C for 2 min, followed by 35 cycles of 94˚C for 15 sec, 60˚C for 30 sec, and 58˚C for 1.5 min and a final extension step at 68˚C for 10 min. The amplicons were purified using a gel extraction kit and ligated into the pET28a(+) expression vector with a His-tag. Correctly ligated plasmids were transformed into *E. coli* BL21(DE3). The protein expression and purification was performed as described above. *P. knowlesi* MSP1-19 protein was cloned into pGEX-4T-2 vector (GE Healthcare Life Sciences, Uppsala, Sweden) by In-Fusion cloning according to manufacturer's manual, and the cloned pDNAs were transformed into BL21(DE3) competent cells for recombinant protein expression. The proteins were purified with Glutathione Sepharose 4B (GE Healthcare Life Sciences) and used for mice antibody production.

SDS-PAGE and western blot analysis

Parasite lysates were prepared from *P. knowlesi* schizont as described previously [55]. Recombinant proteins were separated by 13% SDS-PAGE under reducing or non-reducing conditions and stained with 0.25% Coomassie brilliant blue R-250 (Sigma-Aldrich) and used for western-blotting analysis [25]. The membrane-transferred proteins were reacted with primary rabbit polyclonal serum (1:50) or an anti-His monoclonal antibody (1:2,000, Hilden, Hamburg, Germany) and then reacted with secondary IRDye-labeled goat anti-rabbit or goat anti-mouse antibodies (1:10,000) (LI-COR Bioscience, Lincoln, NE). An Odyssey infrared imaging system (LI-COR Bioscience) and Odyssey software (LI-COR Bioscience) were used to visualize the bands.

Animal antibody production and IgG purification

All *P. vivax* blood-stage antigen-specific antibodies were obtained during our previous studies (Table 1, S3 Table). Total IgG was purified from 1 mL of rabbit serum by using a protein G HP column according to the manufacturer's protocol (GE Healthcare Life Sciences) as described elsewhere [47]. All animal experimental protocols were approved by the Institutional Ethics Committee and followed the Ethical Guidelines for Animal Experiments of Kangwon National University (KIACUC-16-0158).

Antigen-specific IgG antibody purification from patient serum samples

The serum samples used in this study were pooled from eight *P. vivax*-infected patients from the ROK with a high response to the particular antigen of interest, which was screened by immunoscreening with a protein microarray. The control comprised pooled serum samples from eight healthy individuals from a nonendemic area of the ROK. Total IgG antibodies were purified from the pooled serum samples by using protein G columns according to the manufacturer's protocol (GE Healthcare Life Sciences). The isolated IgG antibodies were dialyzed against RPMI 1640 medium and concentrated using centrifugal devices (Merck Millipore, Darmstadt, Germany) with a 30-kDa cut-off value to a concentration of 10 to 20 mg/mL. PvRBP1a, Pv41, and PvRhopH2 recombinant proteins (2–3 mg each) were immobilized on cyanogen bromide (CNBr)-activated Sepharose 4 fast flow beads (GE Healthcare Life Sciences) according to the manufacturer's instructions. The total isolated IgG antibodies (0.5 mL) was loaded to the column filled with antigen coupled beads and eluted using an elution buffer (0.1 M glycine, pH 2.7). The eluted antigen-specific IgGs were immediately neutralized with a Tris buffer (pH 9.0) and dialyzed against incomplete RPMI 1640 medium to the desired concentration.

Immunofluorescence assay (IFA)

An IFA was performed as described previously [47]. The slides were dual probed with a panel of rabbit polyclonal serum against *P. vivax* antigens (1:50) and mice serum against *P. knowlesi* antigens as localization markers (PkMSP1-19 for merozoite surface, PkDBPα-II for microneme, and PkRhopH2 for rhoptry; 1:50). Alexa Fluor 488 goat anti-mouse IgG (H+L) and Alexa Fluor 568 goat-anti rabbit IgG (H+L) were used as secondary antibodies. Nuclei were stained with 4',6-diamidino-2-phenylindole (DAPI, Invitrogen). Red and green pixel intensities were analyzed by ImageJ. The scatter plots of individual red and green pixel intensities were then compared and coefficient of determination (*r*-squared) was obtained. The larger *r*-squared (as close to 100%) represents the scatter value around the regression line suggesting the variation of red and green pixel intensities around its mean. Colocalization was determined as spatial overlap between red (control) and green pixel intensities as showed in larger *r*-squared value.

Protein microarray

The protein microarray protocol was described elsewhere [25]. Serum was pooled from eight *P. vivax*- and *P. knowlesi*-infected patients, healthy donors and/or individually used without pooling to evaluate cross-immunoreactivity. The pooled or individual *P. vivax*- or *P. knowlesi*-infected patient serum or healthy serum were diluted as 1:25. The cut-off value was equal to the mean fluorescence intensity (MFI) plus two standard deviations (SDs) of the negative samples. Normalized MFI values were calculated from the MFI/cut-off values. The normalized MFI for the pooled patient serum was subtracted from the corresponding normalized MFI for the pooled healthy serum.

Growth inhibition assay

The standardized protocol for the invasion inhibition assay has been described elsewhere [47]. Briefly, 2 mg/mL purified rabbit IgG antibodies, and a concentration gradient of antigen-specific IgG antibodies from patients (0.1, 0.2, and 0.5 mg/mL) was added to a 96-well culture plate containing *P. knowlesi* schizonts with 1.5% initial parasitemia and 2% hematocrit from fresh human erythrocytes. An anti-Fy6 monoclonal antibody (25 μg/mL), which recognizes the 2C3 epitope in the DARC N-terminal region located on the red blood cell surface membrane, was obtained as previously described [56]. This antibody was a kind gift from Dr. Olivier Bertrand and Dr. Yves Colin (Institut National de la Transfusion Sanguine, Paris, France). After 10 h of post-invasion for *P. knowlesi*, the parasites were stained with SYBR Green I (Sigma-Aldrich) and analyzed with an Accuri C6 flow cytometer (Accuri cytometer Inc., Ann Arbor, MI). Two independent experiments were performed in duplicate; three independent experiments in duplicate were not possible due to limited antibody amount.

Data analysis

All calculations and data analysis were performed with GraphPad PRISM 5 (GraphPad Software, Inc., San Diego, CA). The Mann-Whitney test was used to assess differences between means, and one-way ANOVA with Dunnett's test was used to compare the means from more than two groups with control anti-HisGST; 95% confidence intervals (CIs), and $p < 0.05$ was considered significant. The 50% inhibitory concentration (IC_{50}) was plotted against log-transformed antibody concentrations, and curve fitting by nonlinear regression with Excel software was used to identify 50% parasite growth inhibition. Hierarchical clustering was used to calculate the profile of individual seropositivity using TIGR multiarray experiment viewer (MeV) software [57]. The clustering analysis was performed using average linkage clustering with Euclidean distance as a similarity metric.

Results

P. vivax blood-stage antigens are similar to those of *P. knowlesi*

Twenty rabbit antibodies previously generated against 19 *P. vivax* blood-stage vaccine candidates were evaluated for their cross-species reactivity against *P. knowlesi* (S1 Fig). Of those, most of the *P. vivax* antigens were highly expressed, and previous studies localized 8 to the merozoite surface, 5 microneme molecules, 4 rhoptry molecules, and 2 dense granule molecules (Table 1). The sequence alignment with orthologs of *P. knowlesi* (n = 18) revealed a high degree of similarity, on average 75.2% for *P. vivax* Sal-I and 72.4% for P01 strain., in the regions selected for antibody production (Table 1).

P. vivax blood-stage antigen-specific antibodies bind to *P. knowlesi* antigens

Immunofluorescence assay (IFA) revealed that these antibodies recognized mature schizont- or merozoite stage parasites of *P. knowlesi* (Figs 1–3), whereas antibodies from a PBS-immunized rabbit (NI) and antibody raised against recombinant HisGST protein had no specific reactivity to *P. knowlesi* parasites (Fig 3B). For the analysis of cross-reactivity to the surface antigen of *P. vivax* merozoites, anti-PvMSP1-19, anti-PvMSP1P-19, anti-PvMSA180-N, anti-PvMSA180-C, anti-Pv41, anti-PvMSP8, anti-PvMSP10, anti-Pv50, and anti-Pv32 antibodies were used. Most of the surface antigens in *P. knowlesi* parasites were highly cross-reactive with the 9 *P. vivax* antibodies and a positive control anti-PkMSP1-19 antibody (Fig 1). The anti-PvMSP1-19 and PvMSA180-N antibody showed the strongest recognition of the surface of the *P. knowlesi* merozoite, as shown by full overlap ($r^2 > 95\%$) with the anti-PkMSP1-19 signals (Fig 1, S1 Table).
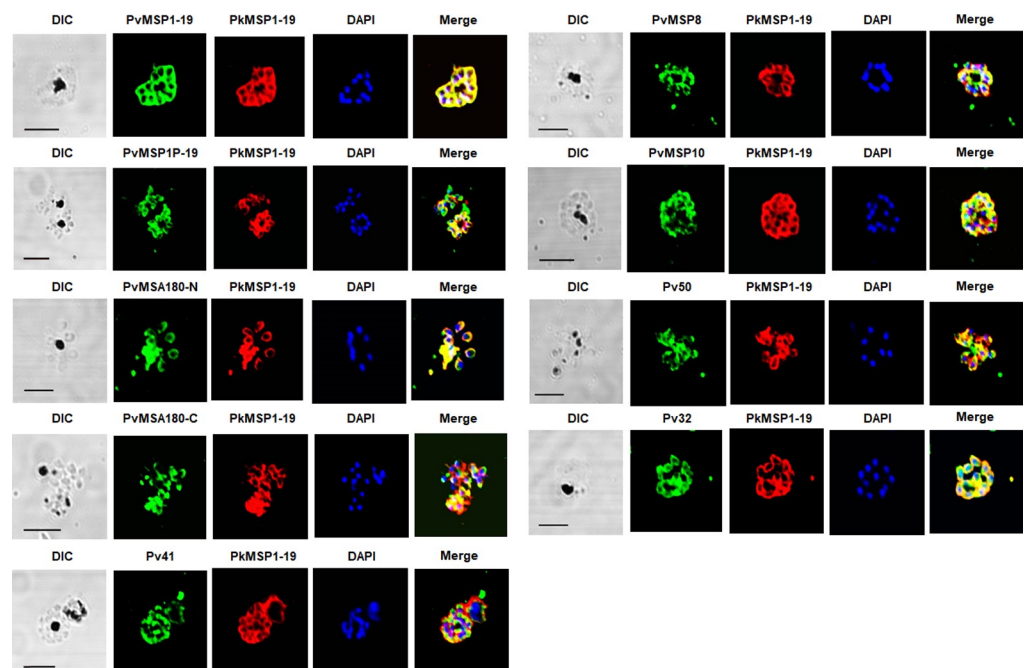

Fig 1. Cross-species reactivity of antibodies against *P. vivax* merozoite surface proteins to *P. knowlesi* parasites by immunofluorescence assay. Localization of a panel of antibodies for *P. vivax* surface proteins (green) in *P. knowlesi* co-stained with anti-PkMSP1-19 (red) as a surface marker. DIC, differential interference contrast; DAPI, 4',6-diamidino-2-phenylindole (blue). All parasites shown are segmented schizonts (24–28 hours post-invasion). Bars indicate 5 μm.
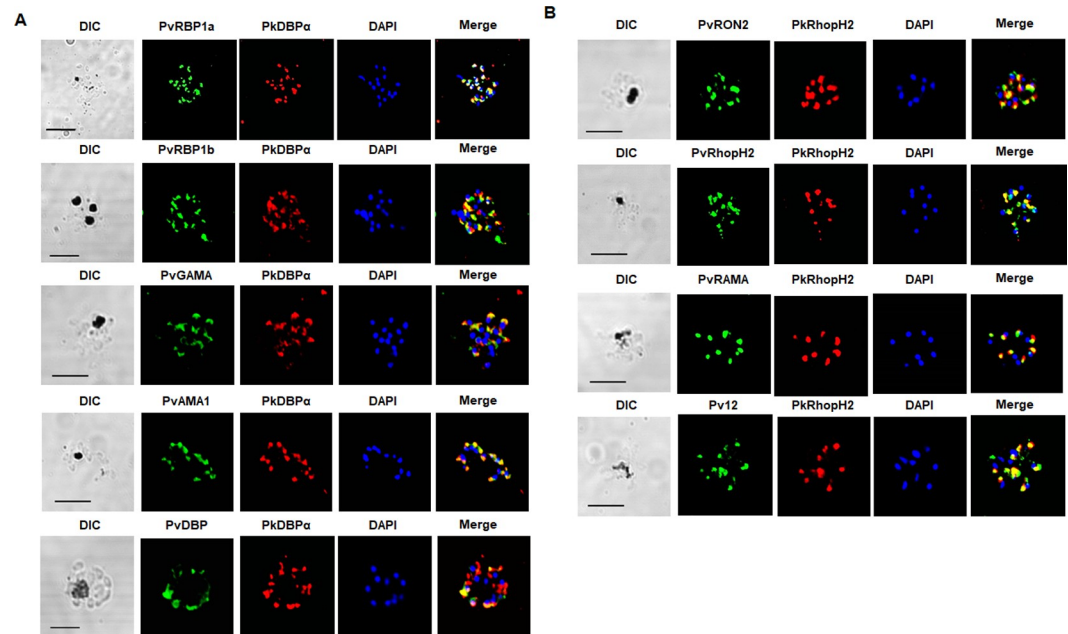
https://doi.org/10.1371/journal.pntd.0008323.g001

Fig 2. Cross-species reactivity of antibodies against *P. vivax* apical organelles proteins to *P. knowlesi* parasites by immunofluorescence assay. (A) Localization of a panel of antibodies for *P. vivax* micronemal proteins (green) in *P. knowlesi* co-stained with anti-PkDBPα (red) as a microneme marker and DAPI as nuclear marker (blue). (B) Localization of a panel of antibodies for *P. vivax* rhoptry proteins (green) in *P. knowlesi* co-stained with anti-PkRhopH2 (red) as a rhoptry marker and DAPI as nuclear marker (blue). All parasites shown are segmented schizonts (24–28 hours post-invasion). Bars indicate 5 μm.

https://doi.org/10.1371/journal.pntd.0008323.g002

Most signals with antibodies against *P. vivax* microneme proteins, PvRBP1a, PvRBP1b, PvGAMA, PvAMA1, and PvDBP, were colocalized with signals with anti-micronemal PkDBPα antibody in *P. knowlesi* parasites (Fig 2A). Interestingly, antibodies against PvRBP1a and PvRBP1b, for which the syntenic orthologs are pseudogenes in *P. knowlesi*, showed signals for these parasites (Fig 2A).

Antibodies against *P. vivax* rhoptry body antigens (PvRhopH2) and rhoptry neck antigens (PvRON2) cross-reacted with *P. knowlesi* showing complete (PvRhopH2) or partial (others) colocalization signals for rhoptry body protein PkRhopH2 in *P. knowlesi* parasites, respectively (Fig 2B, S1 Table). Antibodies against PvETRAMP11.2 and PvEXP1, which localize to the parasitophorous vacuole/dense granules, partially overlapped with the MSP1-19 (surface) consistent with a parasitophorous vacuole localization (Fig 3A). The western blot analysis using parasite lysates showed that the *P. vivax* antibodies also recognized bands at expected full-length sizes or probably the processing proteins (S2 Fig). PvMSP1-19 and PvRhopH2 antibodies were surprisingly recognized the full length of MSP1 protein in *P. knowlesi* lysate. However, non- specific recognition was seen in PvETRAMP11.2 which is in line that the PvE-TRAMP11.2 antibody did not cross-react with *P. knowlesi* parasite organelle protein, but did recognize the parasite membrane.

Antibodies raised against *P. vivax* blood-stage antigens inhibited the erythrocyte invasion by *P. knowlesi*

We next investigated if antibodies raised against *P. vivax* antigens block human erythrocyte invasion by *P. knowlesi* in vitro. We found that the invasion of *P. knowlesi* was inhibited by all antibodies except RON2 when 2 mg/mL of *P. vivax* rabbit polyclonal IgG were administered
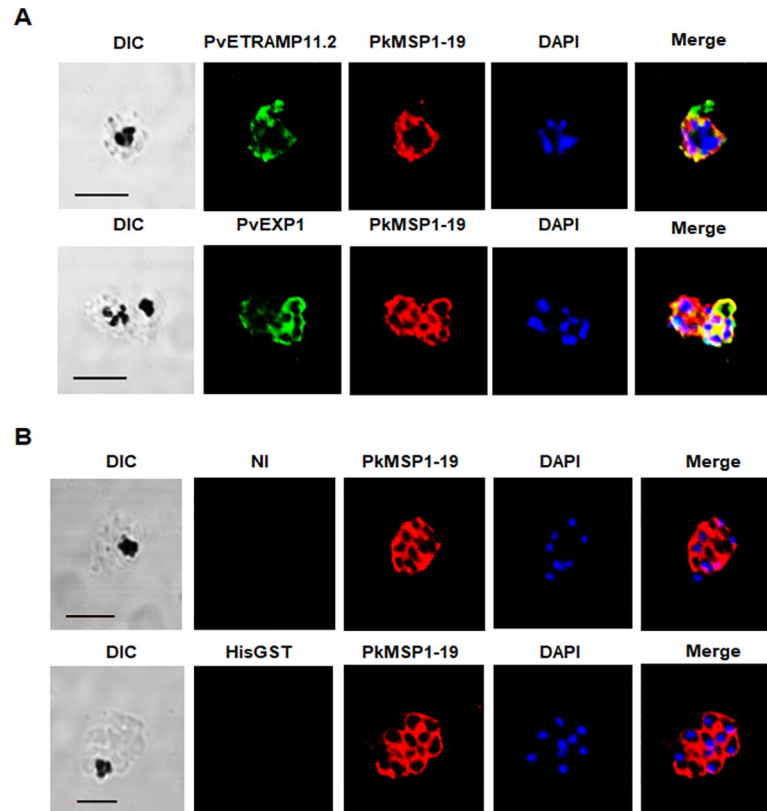
Fig 3. Cross-species reactivity of antibodies against *P. vivax* parasitophorous vacuole membrane molecules and negative control antibodies to *P. knowlesi* parasites by immunofluorescence assay. (A) Localization of antibodies for *P. vivax* parasitophorous vacuole proteins (green) in *P. knowlesi* co-stained with anti-PkMSP1-19 as a merozoite surface marker. (B) Localization of PBS-immunized (NI) and HisGST antibodies to *P. knowlesi*. All parasites shown are segmented schizonts (24–28 hours post-invasion). Bars indicate 5 µm.

https://doi.org/10.1371/journal.pntd.0008323.g003

(Fig 4). The inhibition levels varied between the different antigens, but several were higher than 60% (P41, MSP10, P50, RBP1a, RBP1b). Mild inhibition with dose-dependen manner was observed with PvMSP1-19 and PvAMA1 antibodies (Fig 4, S3 Fig). The negative control antibodies, anti-HisGST and PBS-immunized rabbit IgG (anti-NI) showed little to no inhibition, respectively. Administration of 2C3 monoclonal antibody, which targets Duffy antigens on the erythrocyte, resulted in a high degree of inhibition (92.8 ± 1.6%) (Fig 4). Control antibodies, anti-PkDBPα, and anti-PkAMA1 antibodies showed inhibition activity with dose-dependent manner as described in our previous study [47] (S3 Fig).

To determine whether these antibodies demonstrate additive erythrocyte invasion inhibition, a combination of antibodies against three different antigens localized on the surface (Pv41), microneme (PvRBP1a), and rhoptry (PvRhopH2) were combined in a total concentration of 2 mg/mL and evaluated. We found that a combination of these antibodies significantly increased the invasion inhibition efficacy than single antibodies (S4 Fig).

Human antibodies against *P. vivax* blood-stage antigens inhibit erythrocyte invasion by *P. knowlesi*

To confirm the cross-species inhibition activity of antibodies against *P. vivax* antigens, we examined whether human antibodies against the *P. vivax* antigens in the serum of patients naturally exposed to *P. vivax* infection could inhibit *P. knowlesi* erythrocyte invasion. Three *P.*
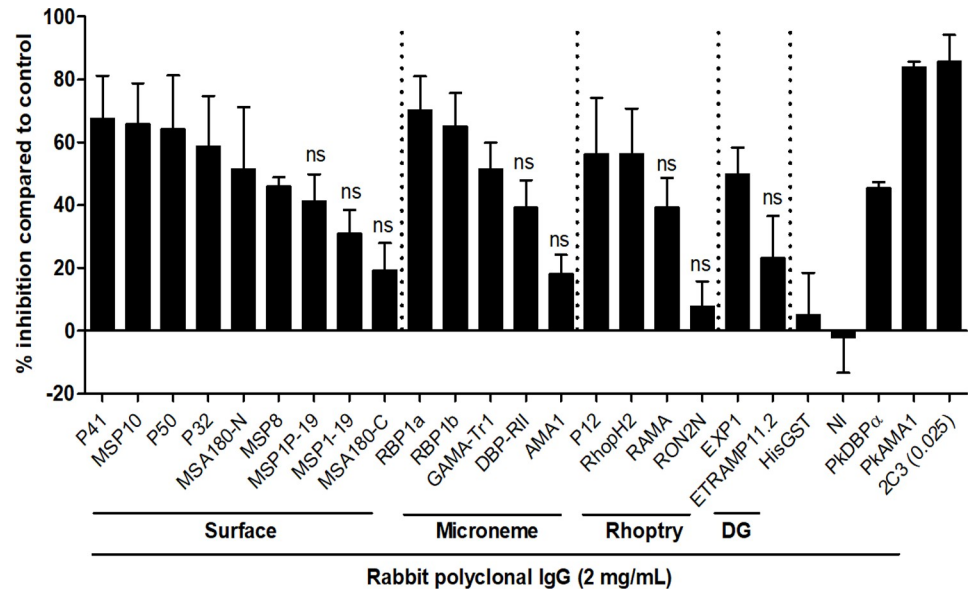
Fig 4. Cross-species activity of antibodies against *P. vivax* antigens to inhibit erythrocyte invasion by *P. knowlesi* parasites. Graph showing inhibition activity (%) of antibodies against *P. vivax* antigens to erythrocyte invasion by *P. knowlesi* A1-H.1 (2 mg/mL rabbit IgG). PkDBPα, PkAMA1 rabbit polyclonal IgG, and 2C3 monoclonal antibody served as control. NI, PBS-immunized rabbit IgG; DG, dense granules; 2C3, Anti-Fy6 monoclonal antibody (25 μg/mL). Graphs show the mean and error bars denote ±1 SD of duplicate test wells in two independent experiments by using one-way ANOVA with Dunnett's multiple comparison test of means of antibody inhibition rate with mean of control anti-HisGST. ns, no significant difference, $p > 0.05$.

https://doi.org/10.1371/journal.pntd.0008323.g004

vivax antigens, PvRBP1a, Pv41, and PvRhopH2 (Fig 5A and 5B) were successfully produced and used for immobilizing on CNBr beads to purify antigen-specific IgGs from the serum of *P. vivax*-infected patients. These antigens were selected because each of them exhibited the highest inhibitory activities within the same localization group (merozoite surface, microneme, or rhoptry). The folded and unfolded PvRBP1a was then reacted with *P. vivax*-infected patients serum, and showed reduction of positive reactivity to unfolded protein as compared to folded PvRBP1a. It suggested that the protein was also successfully refolded (S5 Fig). The patients living in vivax malaria endemic area in the Republic of Korea, would have had no previous exposure to *P. knowlesi* and were used to purify those three antigens specific human IgG. Anti-Pv41- and anti-PvRhopH2-specific IgGs showed a concentration-dependent invasion inhibition activity to *P. knowlesi*, whereas anti-PvRBP1a-specific IgG showed a very little inhibition activity to *P. knowlesi* compared to naïve human IgG (Fig 5C).

Serum from knowlesi- or vivax-malaria patients recognized a panel of vivax- and knowlesi recombinant proteins

To determine the cross-reactivity in malaria patients living in an endemic area, cross- immunoreactivity of antibodies from *P. knowlesi*- or *P. vivax*-infected patients was assessed using a protein microarray of vivax and knowlesi-recombinant proteins. Serum from vivax- and knowlesi-infected malaria patients recognized recombinant *P. vivax* and/or *P. knowlesi* proteins at different levels of reactivity (Fig 6). PvMSP8 and PvMSA180-N recombinant antigens are found to be more reactive to pooled *P. knowlesi*-infected serum (Fig 6A), while Pk50 was very reactive to pooled *P. vivax*-infected serum (Fig 6B).

To further investigate the individual immunoprofiling for cross-reactivity, three *P. knowlesi* recombinant proteins were used. Three most reactive antigens were selected from
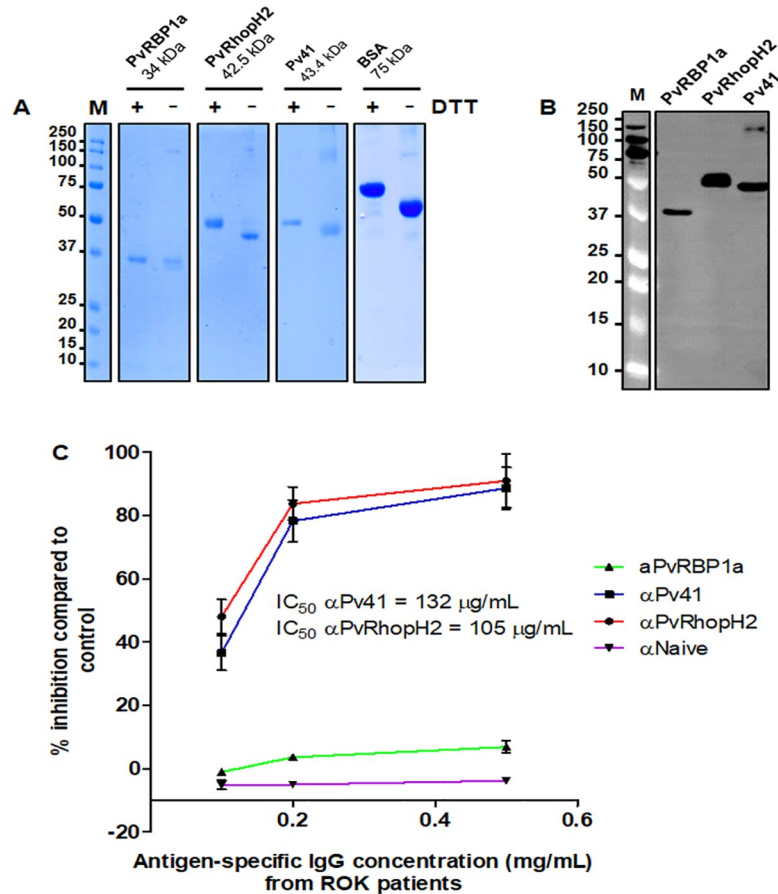
Fig 5. Growth inhibition activity of antigen-specific IgG from *P. vivax*-infected patients to *P. knowlesi* parasites.
(A) Different migration on SDS-PAGE of reduced and non-reduced recombinant proteins immobilized on agarose beads. Proteins were successfully refolded as shown with Coomassie Brilliant Blue in different migration patterns with and without DTT treatment. BSA was served as control. Proteins were then used for immobilization with CNBr-bead for antigen-specific antibody purification from *P. vivax*-infected patients serum. (B) Western blot analysis of recombinant PvRBP1a, PvRhopH2, and Pv41 proteins with anti-His-tag antibody. (C) Growth inhibition activity of IgGs specific to *P. vivax* antigens to *P. knowlesi*. Different concentration of antigen-specific antibodies from human (Pv41, PvRhopH2, PvRBP1a) ranging from 0.1, 0.2 and 0.5 mg/mL were used. IC50 of Pv41 antigen-specific human antibodies was higher than PvRhopH2 antigen-specific human antibodies. αNaive indicates IgG purified healthy individual who have never experienced malaria infection.

https://doi.org/10.1371/journal.pntd.0008323.g005

immunoscreening results using pooled serum (Fig 6B, S6 Fig). The mean average of seropositive rate of these three antigens was higher to *P. knowlesi*-infected patient serum (61.9%) than *P. vivax*-infected patient serum (43.3%) (Fig 7, Table 2). Of those, the PkMSA180-N is the most reactive to *P. knowlesi*- and *P. vivax*-infected patient serum; 77.1 and 51.4%, respectively (Table 2). In total, 37.1% (26/70) of *P. knowlesi*-infected patients showed seropositive to all three *P. knowlesi* antigens and 27.1% (19/70) of *P. vivax*-infected patients showed seropositive to all three *P. knowlesi* antigens (S7 Fig). This data indicates that these three proteins are highly immunogenic and posses shared/common epitopes in the two species.

Discussion

Mixed infections are frequently discussed in the context of parasite-parasite interactions among different *Plasmodium* spp. and a high degree of amino acid sequence similarity and shared common epitopes for some parasites antigens suggests a potential role for cross-species
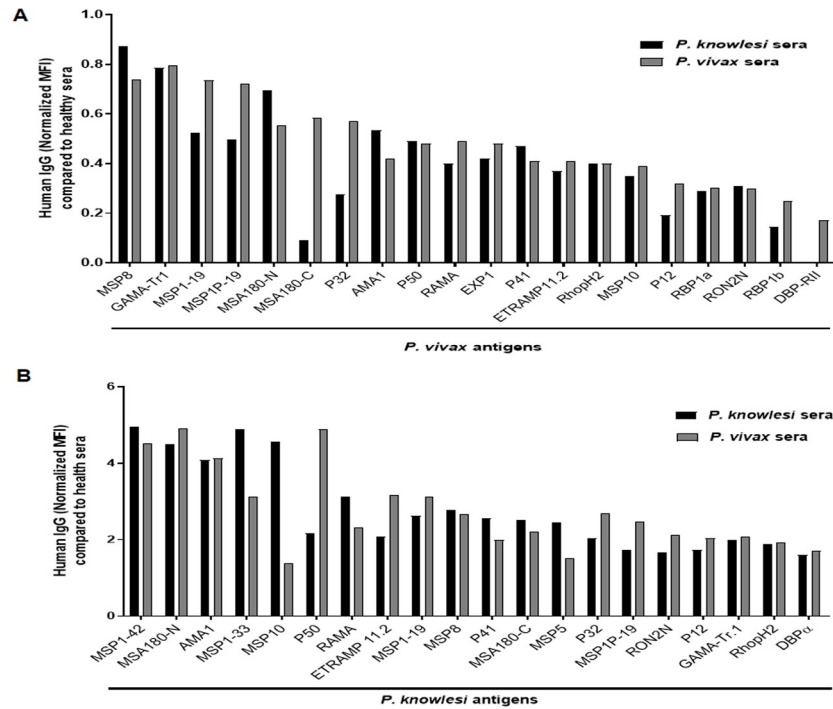
Fig 6. Cross-species reactivity of sera from *P. knowlesi*- and *P. vivax*-malaria clinical patients against *P. vivax* and/ or *P. knowlesi* proteins. (A) IgG responses of pooled *P. vivax*-infected patient serum from the Republic of Korea (ROK) and knowlesi-infected patient serum (Malaysia) with *P. vivax* recombinant proteins after subtraction with pooled healthy serum tier in 1:25 dilution. (B) IgG responses of pooled *P. vivax*-infected patient serum from the Republic of Korea (ROK) and *P. knowlesi*-infected patient serum (Malaysia) with *P. vivax* recombinant proteins.

immunity [21]. A proof-of-concept study in our laboratory reported that cross-species reactivity between *P. vivax* and *P. knowlesi* was observed for an apical asparagine-rich protein [25]. In the current study, we characterized antibodies against 20 recombinant proteins derived from 19 *P. vivax* blood-stage vaccine candidates for their cross-reactivity to *P. knowlesi*. Genome analysis of *P. knowlesi* revealed approximately 80% of genes that are orthologous to *P. vivax*, *P. falciparum*. Among the 19 blood-stage antigens, we selected domains for expression based on their importance for immune response or host cell receptor recognition that we have found in our previous studies (Table 1). Whilst the majority of these had direct orthologues in *P. knowlesi*, some did not, including PvRBP1a and PvRBPb which are found as pseudogenes in the *P. knowlesi*.

We observed the antibodies against *P. vivax* antigens showed the expected localization pattern for the surface or apical organelles of *P. knowlesi* based on the localization information on *P. vivax*. Complete surface colocalization was observed with the anti-PvMSP1-19 antibody in *P. knowlesi*, consistent with the 82.6% amino acid identities of PvMSP1-19 to orthologs of *P. knowlesi* MSP1-19 and suggestive to a previous report [21]. Although syntenic orthologs of PvRBP1a and PvRBP1b do not exist in *P. knowlesi*, these antibodies reacted to the apical side of *P. knowlesi* merozoites, suggesting that non-syntenic paralogues were recognized, PkNBPXa or PkNBPXb. Protein similarities may explain this phenomenon as similar protein sequences do not always produce similar protein structures [58,59]. Previous studies supported that the structural similarities observed among *P. falciparum* Erythrocyte membrane protein 1 variants, PvDBP and Variant surface antigen 2-CSA, and PvAMA1 and PfAMA1 were shown to mediate cross-reactivity to a conserved epitope [60–62].
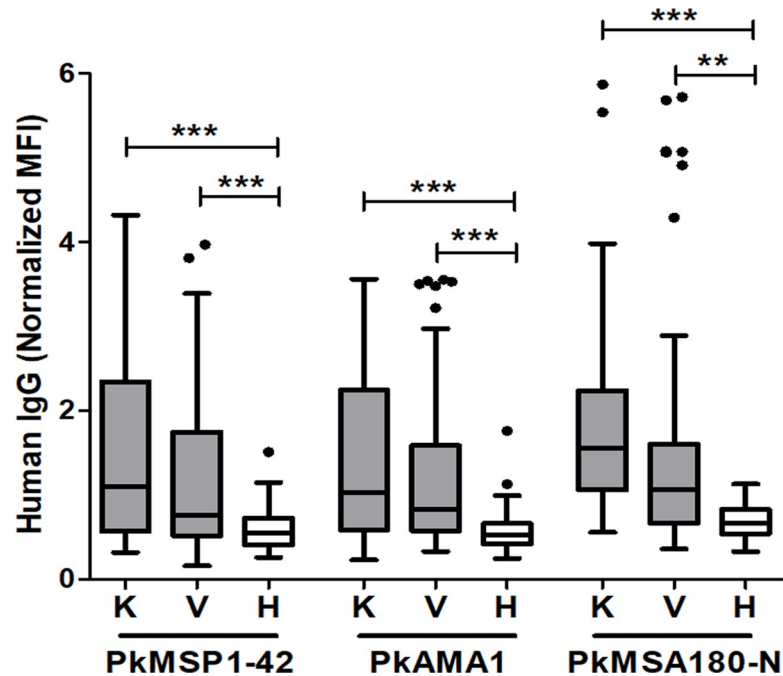
Fig 7. *P. knowlesi* blood-stage cross-reactivity with individual patient serum. The human IgG response of PkMSP1-42, PkMSA180-N, and PkAMA1. Individual with outlier reactivity was indicated in black dot. The prevalence of antibody response was compared to the patients (K, knowlesi; V, vivax) and healthy (H) using the Mann-Whitney test. *** = *p*<0.001.

https://doi.org/10.1371/journal.pntd.0008323.g007

The functional activity of *P. vivax*-specific antibodies against heterologous parasites was also evaluated to determine whether antibodies could inhibit *P. knowlesi* invasion. We found that compared with controls, most of the *P. vivax*-specific antibodies could effectively block the invasion of *P. knowlesi*. Among all the antibodies, the anti-Pv41, anti-PvRBP1a, and anti-

Table 2. Seropositivity of IgG responses to top 3 antigens in *P. knowlesi* and *P. vivax* malaria patients and healthy individuals.

Antigens (*P. knowlesi*)	Sample (*n*)	No. of samples		Sensitivity (%)[a]/ Specificity (%)[b]	95% CI (%)[c]	MFI[d]	P value[e]
		Positive	Negative				
MSP1-42	*P. knowlesi* patient (70)	39	31	55.7[a]/	44.1–66.8	1.59	P <0.0001
	P. vivax patient (70)	29	41	41.4[a]/	30.6–53.1	1.24	P = 0.0008
	Healthy (30)	1	29	96.7[b]	83.3–99.4	0.59	
AMA1	*P. knowlesi* patient (70)	37	33	52.9[a]/	40.0–62.8	1.82	P <0.0001
	P. vivax patient (70)	26	44	41.4[a]/	26.8–48.9	1.49	P <0.0001
	Healthy (30)	1	29	96.7[b]	83.3–99.4	0.68	
MSA180-N	*P. knowlesi* patient (70)	54	16	77.1[a]/	66.1–85.4	1.49	P<0.0001
	P. vivax patient (70)	36	34	51.4[a]/	40.0–62.8	1.27	P = 0.0016
	Healthy (30)	1	29	96.7[b]	83.3–99.4	0.58	

[a] Sensitivity/ seropositivity rate: percentage of positive in malaria patient samples.

[b] Specificity/ seronegativity rate: percentage of negative in healthy samples.

[c] Confidence intervals.

[d] MFI, mean fluorescence intensity was divided by the cutoff value + 2 standard deviations above the MFI of healthy samples.

[e] *P* value, the difference in the total IgG level for each antigen between knowlesi or vivax malaria patients and healthy individuals were calculated with the Mann whitney *U*-test. *P* value of <0.05 was considered statistically significant.

https://doi.org/10.1371/journal.pntd.0008323.t002

PvRhopH2 antibodies appeared to have the highest growth inhibition assay, which is in line with the recognition of either surface or apical organelles of the merozoite by these antibodies. Interestingly, anti-PvAMA1 and anti-PvMSP1-19 antibodies, which also have strong recognition of native and recombinant proteins, did not show high inhibitory activity against human erythrocyte invasion by *P. knowlesi*. This phenomenon was also observed in a previous study [61] in which an anti-PvAMA1 antibody did not inhibit *P. falciparum*, even though immunoassays showed high cross-reactivity to merozoites, and highlights the need for functional characterization of inhibitory activity. Despite the similarity in protein structure, the difference in molecules charges in the MSP1-19 domain results in no functional antibody activity [36]. The small change in the sequence may lead to a change in epitope recognition by changing the affinity and avidity of the antibody due to the loss of the inhibitory effect of epitope-antibody binding [63,64]. On the other hand, this study has limitation that we were not able to perform the reverse-growth inhibition assay using *P. knowlesi* blood-stage antibodies against *P. vivax* parasite, because of lack of long-term in vitro culture system of *P. vivax* parasites. Moreover, the further studies are required to reinforce the cross-species reactivity study.

One of the critical issues of the current malaria vaccine development is the low efficacy, for example, RTS,S vaccine showed only around 30% efficacy against children aged from 6–12 months after administration [65]. Such low protective efficacy would be improved if multiple antigens are used. As compared to an antibody specific for the single antigen, pooled antibodies for three antigens showed the additive effect to inhibit *P. knowlesi* invasion into human erythrocytes. The selection of these antibodies may play a role in this observation, as it was proposed that antibodies against merozoite surface slowed down the invasion to allow antibodies against proteins secreted from microneme and rhoptry to bind their targets [66,67].

Southeast Asia is heavily endemic for *P. vivax*, and recently *P. knowlesi* is also recognized to cause zoonotic human malaria in some regions in this area. Thus it is of interest to know if antibodies against one species could play a role in the cross-protection against other *Plasmodium* species. To this end, we found human IgG against *P. vivax* antigens is able to block the erythrocyte invasion by *P. knowlesi*. Failure to inhibit *P. knowlesi* invasion with anti-PvRBP1a IgG maybe because the epitopes recognized by this antibody were not protective epitopes of PvRBP1a homologs in other *Plasmodium* species. However, the limitation of this study is that we could not purify the knowlesi specific antibodies to perform the invasion inhibition assay because we did not have enough *P. knowlesi*-infected patients' serum at that time.

As part of the importance of cross-reactivity, the immunity produced against other species could be one of the pivotal factors affecting the dynamic change in parasite-parasite interactions. Previous studies have shown that serological cross-reactivity is observed between *P. falciparum* and *P. vivax* and between *P. vivax* and *P. knowlesi* [25,68]. In this study, three different reactivities were observed for pooled *P. knowlesi* and/or *P. vivax* patients serum against *P. vivax* and/or *P. knowlesi* antigens; (1) *P. vivax* patients sera are more reactive than *P. knowlesi* patients sera to *P. vivax* antigens and vice versa, which is expected, (2) *P. knowlesi* patients sera are more reactive than *P. vivax* patients sera to *P. vivax* antigens and vice versa, which may be interpreted that cross-reacting epitopes exist not only in their closest orthologs but also in other members encoded by a multigene family [60] so that the antibody binding sites recognize the unrelated proteins [69], and (3) similar reactivity in both patients sera, which suggests shared common epitopes with the closest orthologs. Surprisingly, this study showed that approximately half of the human clinical patients from endemic area are cross-reactive to *P. knowlesi* MSP1-42, MAS180-N or AMA1. These results are important evidence indicating that immunity established against one *Plasmodium* species is able to cross-react against other *Plasmodium* species through shared common epitopes. However, the regular exposure to different *Plasmodium* species in one particular area may be correlated with the

high reactivity of individual patient serum as it might lead to the accumulation of cross-immune antibodies. It is also noted that some of the *P. vivax*-infected patients possess seropositive to either single *P. knowlesi* antigen or in combination, highlighting the cross-protection antibodies for which some patients in the endemic area develop less severe symptoms or low parasitemia [70].

In the malaria pre-elimination era, the emergence of *P. knowlesi* and other zoonotic *Plasmodium* species are one of the obstacles to successfully control malaria in Southeast Asian countries. Cross-species invasion inhibition activities of antibodies against *P. vivax* shown in this study provides important platform to design multi-component malaria vaccines and suggesting the cross-species immunity affecting the disease dynamic change in Malaysia or endemic area. Some patients in malaria-endemic area might possess different antibodies against different *Plasmodium* species. However, the longevity of the cross-immune antibody is still questioned, whether or not it can be maintained long enough to give a cross-protection when the transmission change.

Supporting information

S1 Fig. Schematic diagrams of *P. vivax* blood-stage antigens with their homologs in *P. knowlesi*. Regions used to raise antibodies are shown in brown boxes with the first and the last amino acid positions at the top of diagram. The characteristic of each target was labeled into different colors or patterns of the diagram with its amino acid position at the top. Four targets (MSP1, MSP1P, MSP8, and MSP10) were identified the EGF-domain at the C-terminal region. The characteristic of each target was obtained from www.plasmodb.org.
(TIF)

S2 Fig. Cross-species reactivity of *P. vivax*-specific antibodies with *P. knowlesi* parasites assessed by western blot analysis. *P. vivax*-specific antibodies recognized *P. knowlesi* parasite lysates. R, uninfected RBCs; P, *P. knowlesi* parasite lysate. The predicted full-length proteins were shown in green, and the possible processing-protein products were indicated with red arrowheads.
(TIF)

S3 Fig. The dose dependent growth inhibition activity of *P. vivax* and *P. knowlesi* antibodies. Growth inhibition activity was evaluated using four different concentration (0.5; 1.0; 1.5 and 2.0/mL) rabbit IgG. The non immunized rabbit IgG and 2C3 monoclonal antibody were served as controls. The dose dependent inhibition of activity of PkDBPα and PkAMA1 antibodies were published online [47].
(TIF)

S4 Fig. Additive effect of combined antibodies against *P. vivax* proteins with different localization to *P. knowlesi*. Growth inhibition activity was evaluated using 0.6 mg/mL rabbit IgG as a single antibody or in combination of 3 antibodies at final 2 mg/mL. The single and combination antibody was compared using one-way ANOVA with Dunnett's test. *** = p value < 0.001.
(TIF)

S5 Fig. The human antibody response to PvRBP1a-F (folded) and PvRBP1a-UF (unfolded) recombinant proteins. The prevalence of seropositivity was compared between patients (P: *P. vivax*-infected patients) and healthy individual (H) using the Mann-Whitney test. * = p value < 0.05; ns = non significant.
(TIF)

S6 Fig. Western blot analysis of protein expression using the wheat germ cell-free analysis. The expression level of each protein was detected by using anti-His tag antibody. Total fraction (T) was then centrifuged to separate the soluble fraction (S) and pellet. A total 10 µL of proteins were loaded in each well. His-tag antibody was used to confirm the positive band in western blotting. The specific band that appears in the total fraction (T) was then said as non-soluble protein. Otherwise soluble protein was showed in a specific band appear in both total fraction and soluble fraction by western blotting.
(TIF)

S7 Fig. Heatmap of antibody response in each individual patient to the three different antigens. (A) Antibody response to the three antigens in individual *P. knowlesi*-infected patients. (B) Antibody response to the three antigens in individual *P. vivax*-infected patients. Hierarchical clustering of individual patients reactivity was showed by a vertical dendrogram. The cluster of antibody reactivity in each patient for the three antigens was created based on the Euclidean distance. The red asterisk indicates the same individual with all three seropositive antigens. The color gradient (from blue to red) indicates the adjusted MFI value of antibody reactivity.
(TIF)

S1 Table. The colocalization of *P. vivax* antibodies and *P. knowlesi* on IFA.
(DOCX)

S2 Table. Summary of cloning primers for *P. knowlesi* recombinant protein expression.
(DOCX)

S3 Table. Summary of *P. vivax* antibodies used in this study.
(DOCX)

Acknowledgments

We are also grateful to Dr. Takafumi Tsuboi, Proteo-Science Center (PROS), Ehime University, Matsuyama, Japan for providing *P. vivax* antigen immune serum samples, and Dr. Olivier Bertrand and Dr. Yves Colin, Institut National de la Transfusion Sanguine, Paris, France for providing the 2C3 monoclonal antibody.

Author Contributions

Conceptualization: Fauzi Muh, Myat Htut Nyunt, Robert W. Moon, Eun-Taek Han.

Data curation: Fauzi Muh, Namhyeok Kim, Myat Htut Nyunt, Osamu Kaneko, Eun-Taek Han.

Formal analysis: Fauzi Muh, Namhyeok Kim.

Funding acquisition: Eun-Taek Han.

Investigation: Fauzi Muh, Namhyeok Kim, Egy Rahman Firdaus, Jin-Hee Han, Mohammad Rafiul Hoque, Eun-Taek Han.

Methodology: Fauzi Muh, Myat Htut Nyunt, Jin-Hee Han, Robert W. Moon, Osamu Kaneko, Eun-Taek Han.

Project administration: Ji-Hoon Park.

Resources: Seong-Kyun Lee, Yee Ling Lau.

Supervision: Myat Htut Nyunt, Robert W. Moon, Osamu Kaneko, Eun-Taek Han.

Validation: Fauzi Muh, Eun-Taek Han.

Visualization: Fauzi Muh, Eun-Taek Han.

Writing – original draft: Fauzi Muh, Eun-Taek Han.

Writing – review & editing: Fauzi Muh, Namhyeok Kim, Myat Htut Nyunt, Egy Rahman Firdaus, Jin-Hee Han, Mohammad Rafiul Hoque, Seong-Kyun Lee, Ji-Hoon Park, Robert W. Moon, Yee Ling Lau, Osamu Kaneko, Eun-Taek Han.

References

1. WHO. World malaria report 2017.

2. Cowman AF, Crabb BS. Invasion of red blood cells by malaria parasites. Cell. 2006; 124: 755–766. https://doi.org/10.1016/j.cell.2006.02.006 PMID: 16497586

3. Frech C, Chen N. Genome comparison of human and non-human malaria parasites reveals species subset-specific genes potentially linked to human disease. PLOS Comput Biol. 2011; 7: e1002320. https://doi.org/10.1371/journal.pcbi.1002320 PMID: 22215999

4. Singh B, Sung LK, Matusop A, Radhakrishnan A, Shamsul SSG, et al. A large focus of naturally acquired *Plasmodium knowlesi* infections in human beings. Lancet. 2004; 363: 1017–1024. https://doi.org/10.1016/S0140-6736(04)15836-4 PMID: 15051281

5. Cox-Singh J, Davis TME, Lee K-S, Shamsul SSG, Matusop A, et al. *Plasmodium knowlesi* malaria in humans is widely distributed and potentially life-threatening. Clin Infect Dis. 2008; 46: 165–171. https://doi.org/10.1086/524888 PMID: 18171245

6. Yusof R, Lau YL, Mahmud R, Fong MY, Jelip J, et al. High proportion of knowlesi malaria in recent malaria cases in Malaysia. Malar J. 2014; 13: 168–168. https://doi.org/10.1186/1475-2875-13-168 PMID: 24886266

7. Lubis IND, Wijaya H, Lubis M, Lubis CP, Divis PCS, et al. Contribution of *Plasmodium knowlesi* to multi-species human malaria infections in North Sumatera, Indonesia. J Infect Dis. 2017; 215: 1148–1155. https://doi.org/10.1093/infdis/jix091 PMID: 28201638

8. White MT, Shirreff G, Karl S, Ghani AC, Mueller I. Variation in relapse frequency and the transmission potential of *Plasmodium vivax* malaria. Proc Biol Sci. 2016; 283: 20160048–20160048. https://doi.org/10.1098/rspb.2016.0048 PMID: 27030414

9. Mayxay M, Pukrittayakamee S, Newton PN, White NJ. Mixed-species malaria infections in humans. Trends Parasitol. 2004; 20: 233–240. https://doi.org/10.1016/j.pt.2004.03.006 PMID: 15105024

10. Putaporntip C, Hongsrimuang T, Seethamchai S, Kobasa T, Limkittikul K, et al. Differential prevalence of *Plasmodium* infections and cryptic *Plasmodium knowlesi* malaria in humans in Thailand. J Infect Dis. 2009; 199: 1143–1150. https://doi.org/10.1086/597414 PMID: 19284284

11. Jiang N, Chang Q, Sun X, Lu H, Yin J, et al. Co-infections with *Plasmodium knowlesi* and other malaria parasites, Myanmar. Emerg Infect Dis. 2010; 16: 1476–1478. https://doi.org/10.3201/eid1609.100339 PMID: 20735938

12. William T, Jelip J, Menon J, Anderios F, Mohammad R, et al. Changing epidemiology of malaria in Sabah, Malaysia: increasing incidence of *Plasmodium knowlesi*. Malar J. 2014; 13: 390. https://doi.org/10.1186/1475-2875-13-390 PMID: 25272973

13. Cox-Singh J, Singh B. Knowlesi malaria: newly emergent and of public health importance? Trends Parasitol. 2008; 24: 406–410. https://doi.org/10.1016/j.pt.2008.06.001 PMID: 18678527

14. Bruce MC, Day KP. Cross-species regulation of *Plasmodium* parasitemia in semi-immune children from Papua New Guinea. Trends Parasitol. 2003; 19: 271–277. https://doi.org/10.1016/s1471-4922(03)00116-8 PMID: 12798085

15. Cooper DJ, Rajahram GS, William T, Jelip J, Mohammad R, et al. *Plasmodium knowlesi* Malaria in Sabah, Malaysia, 2015–2017: ongoing increase in incidence despite near-elimination of the human-only *Plasmodium* species. Clin Infect Dis. 2019.

16. William T, Rahman HA, Jelip J, Ibrahim MY, Menon J, et al. Increasing incidence of *Plasmodium knowlesi* malaria following control of *P. falciparum* and *P. vivax* malaria in Sabah, Malaysia. PLOS Negl Trop Dis. 2013; 7: e2026. https://doi.org/10.1371/journal.pntd.0002026 PMID: 23359830

17. Snounou G, White NJ. The co-existence of *Plasmodium*: sidelights from falciparum and vivax malaria in Thailand. Trends Parasitol. 2004; 20: 333–339. https://doi.org/10.1016/j.pt.2004.05.004 PMID: 15193565

18. Brahimi K, Badell E, Sauzet J-P, BenMohamed L, Daubersies P, et al. Human antibodies against *Plasmodium falciparu*m liver-stage antigen 3 cross-react with *Plasmodium yoelii* preerythrocytic-stage epitopes and inhibit sporozoite invasion in vitro and in vivo. Infect Immun. 2001; 69: 3845–3852. https://doi.org/10.1128/IAI.69.6.3845-3952.2001 PMID: 11349050

19. Kawai S, Hirai M, Haruki K, Tanabe K, Chigusa Y. Cross-reactivity in rapid diagnostic tests between human malaria and zoonotic simian malaria parasite *Plasmodium knowlesi* infections. Parasitol Int. 2009; 58: 300–302. https://doi.org/10.1016/j.parint.2009.06.004 PMID: 19527797

20. Diggs CL, Sadun EH. Serological cross reactivity between *Plasmodium vivax* and *Plasmodium falciparum* as determined by a modified fluorescent antibody test. Exp Parasitol. 1965; 16: 217–223. https://doi.org/10.1016/0014-4894(65)90046-9 PMID: 14281219

21. Woodberry T, Minigo G, Piera KA, Hanley JC, de Silva HD, et al. Antibodies to *Plasmodium falciparum* and *Plasmodium vivax* merozoite surface protein 5 in Indonesia: species-specific and cross-reactive responses. J Infect Dis. 2008; 198: 134–142. https://doi.org/10.1086/588711 PMID: 18471084

22. Maitland K, Williams TN, Newbold CI. *Plasmodium vevax* and *P. falciparum*: Biological interactions and the possibility of cross-species immunity. Parasitol Today. 1997; 13: 227–231. https://doi.org/10.1016/s0169-4758(97)01061-2 PMID: 15275075

23. Goodrich JK, Davenport ER, Waters JL, Clark AG, Ley RE. Cross-species comparisons of host genetic associations with the microbiome. Sci. 2016; 352: 532–535.

24. Benmohamed L, Thomas A, Bossus M, Brahimi K, Wubben J, et al. High immunogenicity in chimpanzees of peptides and lipopeptides derived from four new *Plasmodium falciparum* pre-erythrocytic molecules. Vaccine. 2000; 18: 2843–2855. https://doi.org/10.1016/s0264-410x(00)00068-2 PMID: 10812228

25. Muh F, Ahmed MA, Han JH, Nyunt MH, Lee SK, et al. Cross-species analysis of apical asparagine-rich protein of *Plasmodium vivax* and *Plasmodium knowlesi*. Sci Rep. 2018; 8: 5781. https://doi.org/10.1038/s41598-018-23728-1 PMID: 29636493

26. Smith T, Genton B, Baea K, Gibson N, Narara A, et al. Prospective risk of morbidity in relation to malaria infection in an area of high endemicity of multiple species of *Plasmodium*. Am J Trop Med Hyg. 2001; 64: 262–267. https://doi.org/10.4269/ajtmh.2001.64.262 PMID: 11463113

27. Beeson JG, Kurtovic L, Dobaño C, Opi DH, Chan J-A, et al. Challenges and strategies for developing efficacious and long-lasting malaria vaccines. Sci Transl Med. 2019; 11: eaau1458. https://doi.org/10.1126/scitranslmed.aau1458 PMID: 30626712

28. Tachibana S-I, Sullivan SA, Kawai S, Nakamura S, Kim HR, et al. *Plasmodium cynomolgi* genome sequences provide insight into *Plasmodium vivax* and the monkey malaria clade. Nat Genetics. 2012; 44: 1051. https://doi.org/10.1038/ng.2375 PMID: 22863735

29. Carlton JM, Adams JH, Silva JC, Bidwell SL, Lorenzi H, et al. Comparative genomics of the neglected human malaria parasite *Plasmodium vivax*. Nature. 2008; 455: 757. https://doi.org/10.1038/nature07327 PMID: 18843361

30. Igonet S, Vulliez-Le Normand B, Faure G, Riottot MM, Kocken CHM, et al. Cross-reactivity studies of an anti-*Plasmodium vivax* apical membrane antigen 1 monoclonal antibody: binding and structural characterisation. J Mol Biol. 2007; 366: 1523–1537. https://doi.org/10.1016/j.jmb.2006.12.028 PMID: 17229439

31. Anstey NM, Grigg MJ. Zoonotic malaria: the better you look, the more you find. J Infect Dis. 2018; 219: 679–681.

32. Aurrecoechea C, Brestelli J, Brunk BP, Dommer J, Fischer S, et al. PlasmoDB: a functional genomic database for malaria parasites. Nucleic Acids Res. 2009; 37: D539–D543. https://doi.org/10.1093/nar/gkn814 PMID: 18957442

33. Cheng Y, Wang Y, Ito D, Kong D-H, Ha K-S, et al. The *Plasmodium vivax* merozoite surface protein 1 paralog is a novel erythrocyte-binding ligand of *P. vivax*. Infect Immun. 2013; 81: 1585–1595. https://doi.org/10.1128/IAI.01117-12 PMID: 23460511

34. Ahmed MA, Fauzi M, Han ET. Genetic diversity and natural selection of *Plasmodium knowlesi* merozoite surface protein 1 paralog gene in Malaysia. Malar J. 2018; 17: 115. https://doi.org/10.1186/s12936-018-2256-y PMID: 29540177

35. Chen JH, Wang Y, Ha KS, Lu F, Suh IB, et al. Measurement of naturally acquired humoral immune responses against the C-terminal region of the *Plasmodium vivax* MSP1 protein using protein arrays. Parasitol Res. 2011; 109: 1259–1266. https://doi.org/10.1007/s00436-011-2370-z PMID: 21487779

36. Garman SC, Simcoke WN, Stowers AW, Garboczi DN. Structure of the C-terminal domains of merozoite surface protein-1 from *Plasmodium knowlesi* reveals a novel histidine binding site. J Biol Chem. 2003; 278: 7264–7269. https://doi.org/10.1074/jbc.M210716200 PMID: 12493733

37. Cheng Y, Wang B, Sattabongkot J, Lim CS, Tsuboi T, et al. Immunogenicity and antigenicity of *Plasmodium vivax* merozoite surface protein 10. Parasitol Res. 2014; 113: 2559–2568. https://doi.org/10.1007/s00436-014-3907-8 PMID: 24764159

38. Pacheco MA, Elango AP, Rahman AA, Fisher D, Collins WE, et al. Evidence of purifying selection on merozoite surface protein 8 (MSP8) and 10 (MSP10) in *Plasmodium* spp. Infect Genetics Evol. 2012; 12: 978–986.

39. Cheng Y, Wang B, Changrob S, Han JH, Sattabongkot J, et al. Naturally acquired humoral and cellular immune responses to *Plasmodium vivax* merozoite surface protein 8 in patients with *P. vivax* infection. Malar J. 2017; 16: 211. https://doi.org/10.1186/s12936-017-1837-5 PMID: 28532483

40. Cheng Y, Lu F, Tsuboi T, Han ET. Characterization of a novel merozoite surface protein of *Plasmodium vivax*, Pv41. Acta Tropica. 2013; 126: 222–228. https://doi.org/10.1016/j.actatropica.2013.03.002 PMID: 23499861

41. Ahmed MA, Chu K-B, Quan F-S. The *Plasmodium knowlesi* Pk41 surface protein diversity, natural selection, sub population and geographical clustering: a 6-cysteine protein family member. Peer J. 2018; 6: e6141–e6141. https://doi.org/10.7717/peerj.6141 PMID: 30581686

42. Chen JH, Jung JW, Wang Y, Ha KS, Lu F, et al. Immunoproteomics profiling of blood stage *Plasmodium vivax* infection by high-throughput screening assays. J Proteome Res. 2010; 9: 6479–6489. https://doi.org/10.1021/pr100705g PMID: 20949973

43. Cheng Y, Wang B, Lu F, Han JH, Ahmed MA, et al. Immunological characterization of *Plasmodium vivax* Pv32, a novel predicted GPI-anchored merozoite surface protein. Malar J. 2018; 17: 273. https://doi.org/10.1186/s12936-018-2401-7 PMID: 30053874

44. Muh F, Han JH, Nyunt MH, Lee SK, Jeon HY, et al. Identification of a novel merozoite surface antigen of *Plasmodium vivax*, PvMSA180. Malar J. 2017; 16: 133. https://doi.org/10.1186/s12936-017-1760-9 PMID: 28351409

45. Cheng Y, Lu F, Wang B, Li J, Han JH, et al. *Plasmodium vivax* GPI-anchored micronemal antigen (PvGAMA) binds human erythrocytes independent of Duffy antigen status. Sci Rep. 2016; 6: 35581. https://doi.org/10.1038/srep35581 PMID: 27759110

46. Singh S, Pandey K, Chattopadhayay R, Yazdani SS, Lynn A, et al. Biochemical, biophysical, and functional characterization of bacterially expressed and refolded receptor binding domain of *Plasmodium vivax* Duffy-binding Protein. J Biol Chem. 2001; 276: 17111–17116. https://doi.org/10.1074/jbc.M101531200 PMID: 11279211

47. Muh F, Lee SK, Hoque MR, Han JH, Park JH, et al. In vitro invasion inhibition assay using antibodies against *Plasmodium knowlesi* Duffy binding protein alpha and apical membrane antigen protein 1 in human erythrocyte-adapted *P. knowlesi* A1-H.1 strain. Malar J. 2018; 17: 272. https://doi.org/10.1186/s12936-018-2420-4 PMID: 30049277

48. Han JH, Lee SK, Wang B, Muh F, Nyunt MH, et al. Identification of a reticulocyte-specific binding domain of *Plasmodium vivax* reticulocyte-binding protein 1 that is homologous to the PfRh4 erythrocyte-binding domain. Sci Rep. 2016; 6: 26993. https://doi.org/10.1038/srep26993 PMID: 27244695

49. Li J, Ito D, Chen JH, Lu F, Cheng Y, et al. Pv12, a 6-Cys antigen of *Plasmodium vivax*, is localized to the merozoite rhoptry. Parasitol Int. 2012; 61: 443–449. https://doi.org/10.1016/j.parint.2012.02.008 PMID: 22394409

50. Lu F, Li J, Wang B, Cheng Y, Kong DH, et al. Profiling the humoral immune responses to *Plasmodium vivax* infection and identification of candidate immunogenic rhoptry-associated membrane antigen (RAMA). J Proteomics. 2014; 102: 66–82. https://doi.org/10.1016/j.jprot.2014.02.029 PMID: 24607491

51. Wang B, Lu F, Cheng Y, Li J, Ito D, et al. Identification and characterization of the *Plasmodium falciparum* RhopH2 ortholog in *Plasmodium vivax*. Parasitol Res. 2013; 112: 585–593. https://doi.org/10.1007/s00436-012-3170-9 PMID: 23097184

52. Cheng Y, Lu F, Lee SK, Kong DH, Ha KS, et al. Characterization of *Plasmodium vivax* early transcribed membrane protein 11.2 and exported protein 1. PLOS One. 2015; 10: e0127500. https://doi.org/10.1371/journal.pone.0127500 PMID: 26011536

53. Moon RW, Hall J, Rangkuti F, Ho YS, Almond N, et al. Adaptation of the genetically tractable malaria pathogen *Plasmodium knowlesi* to continuous culture in human erythrocytes. Proc Natl Acad Sci. 2013; 110: 531–536. https://doi.org/10.1073/pnas.1216457110 PMID: 23267069

54. Bhardwaj R, Shakri AR, Hans D, Gupta P, Fernandez-Becerra C, et al. Production of recombinant PvDBPII, receptor binding domain of *Plasmodium vivax* Duffy binding protein, and evaluation of immunogenicity to identify an adjuvant formulation for vaccine development. Prot Expr Purif. 20017; 136: 52–57.

55. Boddey JA, Moritz RL, Simpson RJ, Cowman AF. Role of the *Plasmodium* export element in trafficking parasite proteins to the infected erythrocyte. Traffic. 2009; 10: 285–299. https://doi.org/10.1111/j.1600-0854.2008.00864.x PMID: 19055692

56. Wasniowska K, Petit-LeRoux Y, Tournamille C, Le van Kim C, Cartron JP, et al. Structural characterization of the epitope recognized by the new anti-Fy6 monoclonal antibody NaM185-2C3. Transfus Med. 2002; 12: 205–211. https://doi.org/10.1046/j.1365-3148.2002.00373.x PMID: 12164140

57. Saeed AI, Sharov V, White J, Li J, Liang W, et al. TM4: a free, open-source system for microarray data management and analysis. BioTechniques. 2003; 34: 374–378. https://doi.org/10.2144/03342mt01 PMID: 12613259

58. Vulliez-Le Normand B, Saul FA, Hoos S, Faber BW, Bentley GA. Cross-reactivity between apical membrane antgen 1 and rhoptry neck protein 2 in *P. vivax* and *P. falciparum*: A structural and binding study. PLOS One. 2017; 12: e0183198. https://doi.org/10.1371/journal.pone.0183198 PMID: 28817634

59. Douradinha B, Mota MM, Luty AJF, Sauerwein RW. Cross-species immunity in malaria vaccine development: two, three, or even four for the price of one?. Infect Immun. 2008; 76: 873–878. https://doi.org/10.1128/IAI.00431-07 PMID: 18056479

60. Gnidehou S, Mitran CJ, Arango E, Banman S, Mena A, et al. Cross-species immune recognition between *Plasmodium vivax* Duffy Binding Protein Antibodies and the *Plasmodium falciparum* Surface Antigen VAR2CSA. J Infect Dis. 2018; 219: 110–120.

61. Drew DR, Sanders PR, Weiss G, Gilson PR, Crabb BS, et al. Functional conservation of the ama1 host-cell invasion ligand between *P. falciparum* and *P. vivax*: A novel platform to accelerate vaccine and drug development. J Infect Dis. 2018; 217: 498–507. https://doi.org/10.1093/infdis/jix583 PMID: 29165651

62. Klein MM, Gittis AG, Su H-P, Makobongo MO, Moore JM, et al. The cysteine-rich interdomain region from the highly variable *Plasmodium falciparum* erythrocyte membrane protein-1 exhibits a conserved structure. PLOS Pathog. 2008; 4: e1000147. https://doi.org/10.1371/journal.ppat.1000147 PMID: 18773118

63. Mamillapalli A, Sunil S, Diwan SS, Sharma SK, Tyagi PK, et al. Polymorphism and epitope sharing between the alleles of merozoite surface protein-1 of *Plasmodium falciparum* among Indian isolates. Malar J. 2007; 6: 95. https://doi.org/10.1186/1475-2875-6-95 PMID: 17659072

64. Vulliez-Le Normand B, Faber BW, Saul FA, van der Eijk M, Thomas AW, et al. Crystal structure of *Plasmodium knowlesi* apical membrane antigen 1 and its complex with an invasion-inhibitory monoclonal antibody. PLOS One. 2015; 10: e0123567. https://doi.org/10.1371/journal.pone.0123567 PMID: 25886591

65. Mahmoudi S, Keshavarz H. Efficacy of phase 3 trial of RTS, S/AS01 malaria vaccine: The need for an alternative development plan. Human Vaccines Immunother. 2017; 13: 2098–2101.

66. Saul A. Kinetic constraints on the development of a malaria vaccine. Parasite Immunol. 1987; 9: 1–9. https://doi.org/10.1111/j.1365-3024.1987.tb00483.x PMID: 2436129

67. Bustamante LY, Powell GT, Lin YC, Macklin MD, Cross N, et al. Synergistic malaria vaccine combinations identified by systematic antigen screening. Proc Natl Acad Sci. 2017; 114: 12045–12050. https://doi.org/10.1073/pnas.1702944114 PMID: 29078270

68. Drew DR, O'Donnell RA, Smith BJ, Crabb BS. A common cross-species function for the double epidermal growth factor-like modules of the highly divergent *Plasmodium* surface proteins MSP-1 and MSP-8. J Biol Chem. 2004; 279: 20147–20153. https://doi.org/10.1074/jbc.M401114200 PMID: 14976193

69. Frank SA. Immunology and Evolution of Infectious Disease. Princeton (NJ). 2002.

70. Ahmed AM, Pinheiro MM, Divis PC, Siner A, Zainudin R, et al. Disease progression in *Plasmodium knowlesi* malaria is linked to variation in invasion gene family members. PLOS Negl Trop Dis. 2014; 8: e3086. https://doi.org/10.1371/journal.pntd.0003086 PMID: 25121807